Encyclopedia of emergent particles in 528 magnetic layer groups and 394 magnetic rod groups

Zeying Zhang [1,2] Weikang Wu [3,4,*] Gui-Bin Liu,[5,6] Zhi-Ming Yu [5,6] Shengyuan A. Yang [2,†] and Yugui Yao[5,6,‡]

[1]*College of Mathematics and Physics, Beijing University of Chemical Technology, Beijing 100029, China*
[2]*Research Laboratory for Quantum Materials, Singapore University of Technology and Design, Singapore 487372, Singapore*
[3]*Key Laboratory for Liquid-Solid Structural Evolution and Processing of Materials, Ministry of Education, Shandong University, Jinan 250061, China*
[4]*Shenzhen Research Institute of Shandong University, Shenzhen, Guangdong 518057, China*
[5]*Centre for Quantum Physics, Key Laboratory of Advanced Optoelectronic Quantum Architecture and Measurement (MOE), Beijing Institute of Technology, Beijing 100081, China*
[6]*Beijing Key Lab of Nanophotonics & Ultrafine Optoelectronic Systems, School of Physics, Beijing Institute of Technology, Beijing 100081, China*

(Received 24 October 2022; accepted 18 January 2023; published 6 February 2023)

We present a systematic classification of emergent particles in all 528 magnetic layer groups and 394 magnetic rod groups, which describe two-dimensional and one-dimensional crystals, respectively. Our approach is via constructing a correspondence between a given magnetic layer/rod group and one of the magnetic space groups, such that all irreducible representations of the layer/rod group can be derived from those of the corresponding space group. Based on these group representations, we explicitly construct the effective models for possible band degeneracies and identify all emergent particles, including both spinless and spinful cases. We find that there are six kinds of particles protected by magnetic layer groups and three kinds by magnetic rod groups. Our work provides a useful reference for the search and design of emergent particles in lower dimensional crystals.

DOI: 10.1103/PhysRevB.107.075405

I. INTRODUCTION

The research on topological semimetals in the past decade has driven extensive efforts in understanding various emergent particles enabled by the crystalline symmetry [1–3]. In these crystals, novel kinds of quasiparticle states emerge around band degeneracies in the momentum space and their physical properties are determined by the character of the band degeneracies. For example, Weyl and Dirac particles can be realized around twofold and fourfold band nodal points in crystals, known as Weyl and Dirac points, respectively [3–6]. These notions are not limited to electronic systems of real materials, but also extended to many artificial crystals such as acoustic/photonic crystals [7–9], electric circuit arrays [10–12], and mechanical networks [13,14].

A main task in this research is to classify all possible types of emergent particles. The classification is typically based on the dimension of the degeneracy manifold, the degree of degeneracy, the band dispersion, and the topological charge. For instance, in three dimensions (3D), besides nodal points, the band degeneracies may also form nodal lines [15–18] or nodal surfaces [19–21], the degeneracy for a nodal point could be 2, 3, 4, 6, and 8 [22–25], the emergent particle may have linear, quadratic, or cubic dispersion [26–29], and they could have a maximal chiral charge of four [25,30]. All these properties are eventually determined by the symmetry of the bands that form the degeneracy or, more specifically, how these bands represent the symmetry group of the system. For 3D crystals, the pertinent symmetry groups are the (magnetic) space groups. Their (co)representations have been extensively studied and well documented in the past [31] (in the remainder of this paper the "representation" means representation for unitary group and corepresentation for magnetic group). Based on the knowledge of space group representations, an encyclopedia of emergent particles in 3D crystals has been established in recent works [25,32–35].

Recent years also witnessed a rapid development in the realization of low-dimensional crystals. Many 2D layered materials and 1D (or quasi-1D) crystals have been synthesized in experiment [36–38]. Because lower dimensions permit a high controllability and easier detection, emergent particles may have even stronger impact in these systems. As a prominent example, many intriguing properties of graphene can be attributed to its emergent Dirac fermions [39]. So far, there have been works on studying specific kinds of emergent particles in 2D [40] and on systematic construction of $k \cdot p$ models for 2D systems [35,41,42]. However, a comprehensive classification for all emergent particles in magnetic layer groups (MLGs) and magnetic rod groups (MRGs), which apply for 2D and 1D crystals, respectively, has not been achieved.

One obstacle here is that the irreducible representations (IRRs) have not been completely derived for these groups, but only for certain subgroups (such as magnetic line groups and type-I and type-II MLGs [43–46]). In this work, we develop an approach to compute IRRs for all 528 MLGs and

*weikang_wu@sdu.edu.cn
†shengyuan_yang@sutd.edu.sg
‡ygyao@bit.edu.cn

TABLE I. Emergent particles in MLGs. "√" ("×") means the corresponding emergent particle can (cannot) exist in the specified type of magnetic subperiodic groups. d_m is the dimension of the degeneracy manifold. d is the degree of degeneracy. Ld is the leading order dispersion of the band splitting near the degeneracy. "I" to "IV" represent the four types of magnetic subperiodic groups.

Notation	Abbr.	d_m	d	Ld	I	II	III	IV
MLGs w/o spin								
Linear Weyl point	LWP	0	2	(11)	√	√	√	√
Quadratic Weyl point	QWP	0	2	(22)	√	√	√	√
Dirac point	DP	0	4	(11)	×	√	√	√
Weyl line	WL	1	2	(1)	√	√	√	√
Weyl line net	WLs	1	2	(1)	√	√	√	√
MLGs w/ spin								
Linear Weyl point	LWP	0	2	(11)	√	√	√	√
Quadratic Weyl point	QWP	0	2	(22)	√	×	√	×
Cubic Weyl point	CWP	0	2	(33)	√	√	×	×
Dirac point	DP	0	4	(11)	√	√	√	√
Weyl line	WL	1	2	(1)	√	√	√	√
Weyl line net	WLs	1	2	(1)	√	√	√	√
Dirac line	DL	1	4	(1)	×	√	√	√
Dirac line net	DLs	1	4	(1)	×	√	√	√

394 MRGs. The approach is based on making a correspondence between a given MLG/MRG and one of the magnetic space groups. We show that all IRRs of the MLG/MRG can be derived by restricting the IRRs of the corresponding space group under a constraint. After obtaining IRRs for these groups, we identify all possible protected band degeneracies and classify the associated emergent particles, for both spinless and spinful systems. We find six kinds of emergent particles in MLGs and three kinds in MRGs, as listed in Table I. Our work offers a comprehensive reference for the investigation of emergent particles in low dimensional crystals.

II. DERIVE IRRS OF SUBPERIODIC GROUPS

MLGs and MRGs are subperiodic groups in 3D, meaning that their translational parts form a 2D or 1D subspace of 3D. Each of their point groups remains one of the 3D crystallographic point groups. To derive their IRRs, one can of course pursue the standard way as in Refs. [31,47], e.g., by studying little cogroups and using the method of projective representations. Here, we shall adopt an alternative approach, in which we obtain the IRRs of a magnetic subperiodic group from a constructed magnetic space group. The reason is twofold. First, IRRs for magnetic space groups are well known and documented in standard references [31]. Once a correspondence is obtained between a (given) subperiodic group and the constructed space group, the IRRs for the subperiodic group can be readily obtained, as we show below. Second, this approach has the benefit of establishing connections between subperiodic groups and space groups. For example, the labeling of IRRs can be naturally inherited from the standard ones for the space groups, allowing users to have coherent understanding of the content.

A. General approach

Our approach is a unified treatment for both MLGs and MRGs. Consider a given subperiodic group $\mathcal{S}$ [48]. We first construct a magnetic space group $\mathcal{G}$ from $\mathcal{S}$. This is done by taking a lattice translation group $\mathcal{N}$, which consists of translations normal to the subspace for $\mathcal{S}$. For a MLG, $\mathcal{N}$ is the 1D lattice translations normal to the plane. For a MRG, $\mathcal{N}$ contains the 2D translations normal to the line. Then the space group $\mathcal{G}$ is constructed as the semidirect product:

$$\mathcal{G} = \mathcal{N} \rtimes \mathcal{S}. \tag{1}$$

Following this construction method, for a given subperiodic group $\mathcal{S}$, we can always construct a *unique* space group $\mathcal{G}$, despite the fact that there is usually more than one space group containing $\mathcal{S}$ as a subgroup. In the Supplemental Material (SM), we present the constructed $\mathcal{G}$ for each MLG and MRG in Table S1 [49].

By definition, $\mathcal{N}$ is a normal subgroup of $\mathcal{G}$ and $\mathcal{S}$ is isomorphic to $\mathcal{G}/\mathcal{N}$, with the isomorphism

$$\phi : s \in \mathcal{S} \mapsto \mathcal{N}s \in \mathcal{G}/\mathcal{N}. \tag{2}$$

Thus to get IRRs of $\mathcal{S}$ is equivalent to obtaining the IRRs of the quotient group $\mathcal{G}/\mathcal{N}$.

Since $\mathcal{G}$ is one of the magnetic space groups, its IRRs are already known (here obtained by using the MSGCorep package) [50,51]. With this information, all IRRs of $\mathcal{S}$ can be obtained from restricting IRRs of $\mathcal{G}$ to $\mathcal{S}$. However, not all IRRs of $\mathcal{G}$ lead to IRRs of $\mathcal{S}$ under restriction. For some IRRs of $\mathcal{G}$, the restriction to its subgroup would lead to reducible representations. What then are the suitable IRRs ρ of $\mathcal{G}$ that we need to consider? From group representation theory, these are the IRRs which satisfy the condition that ker ρ contains $\mathcal{N}$ as a subgroup [52], i.e.,

$$\mathcal{N} \subseteq \ker \rho = \{g \in \mathcal{G} | \rho(g) \text{ is identity matrix}\}. \tag{3}$$

In other words, the normal translations must be represented as the identity matrix in the IRR ρ of $\mathcal{G}$. The restriction of such ρ to $\mathcal{S}$, i.e., $\rho \downarrow \mathcal{S}$, is indeed an IRR of $\mathcal{S}$. This can be easily verified from the corresponding restricted character $\chi \downarrow \mathcal{S}$, where χ is the character of ρ. Recall that a representation ρ of G is an IRR if and only if its character satisfies $\langle \chi, \chi \rangle_G =$

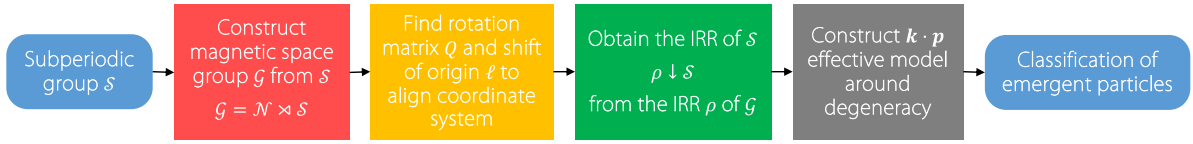

FIG. 1. Flow chart for classification of emergent particles in subperiodic groups.

1; $\langle\theta,\phi\rangle_G$ denotes the inner product of characters for group G. Now, the restricted character $\chi\downarrow\mathcal{S}$ satisfies

$$\begin{aligned}\langle\chi\downarrow\mathcal{S},\chi\downarrow\mathcal{S}\rangle_{\mathcal{S}} &= \frac{1}{|\mathcal{S}|}\sum_{s\in\mathcal{S}}\chi(s)\chi^*(s)\\ &= \frac{1}{|\mathcal{S}||\mathcal{N}|}\sum_{n\in\mathcal{N}}\sum_{s\in\mathcal{S}}\chi(ns)\chi^*(ns)\\ &= \frac{1}{|\mathcal{G}|}\sum_{g\in\mathcal{G}}\chi^*(g)\chi(g) = \langle\chi,\chi\rangle_{\mathcal{G}},\end{aligned}\tag{4}$$

where, in the second step, we used the fact that $\chi(ns)=\chi(s)$ since $\mathcal{N}\subseteq\ker\rho$. Thus the restricted representation $\rho\downarrow\mathcal{S}$ for $\mathcal{S}$ shares the same irreducibility as ρ for $\mathcal{G}$.

In a similar way, one can show that the indicator function for such ρ is also preserved in the process of restriction to $\mathcal{S}$ [47], i.e.,

$$\begin{aligned}\frac{1}{|\mathcal{S}|}\sum_{s\in\mathcal{AS}}\chi(s^2) &= \frac{1}{|\mathcal{S}||\mathcal{N}|}\sum_{n\in\mathcal{N}}\sum_{s\in\mathcal{AS}}\chi((ns)^2)\\ &= \frac{1}{|\mathcal{G}|}\sum_{g\in\mathcal{AG}}\chi(g^2),\end{aligned}\tag{5}$$

where $\mathcal{AS}$ and $\mathcal{AG}$ are the antiunitary parts of $\mathcal{S}$ and $\mathcal{G}$, respectively. In the equation, we used the fact that $\chi((ns)^2)=\chi(nsns)=\chi(nssn')=\chi(s^2)$ with $n'\in\mathcal{N}$ and $\mathcal{N}\subseteq\ker\rho$. This proves that the restricted IRR for $\mathcal{S}$ shares the same type of corepresentation as the original IRR for $\mathcal{G}$.

To illustrate our approach, let us consider the layer group $p6/mmm$ as an example, which is the one for graphene. Following our construction method, we choose group $\mathcal{N}$ containing translations normal to the 2D plane. The semidirect product in Eq. (1) gives a space group $\mathcal{G}$ being $P6/mmm$ (no. 191). Consider the Γ point for $p6/mmm$. One looks for IRRs ρ for $P6/mmm$ such that $\mathcal{N}\subseteq\ker\rho$. This condition is fulfilled only at Γ point of $P6/mmm$ and it turns out that all IRRs there for $P6/mmm$ are also IRRs for $p6/mmm$. In a similar way, IRRs for $p6/mmm$ at K point can be obtained from the IRRs for $P6/mmm$ at K point.

B. Algorithm for aligning coordinate systems

It is not difficult to identify the IRRs of $\mathcal{G}$ that satisfy condition (3). For example, for $\mathcal{S}$ describing a 2D system in the x-y plane, one can easily see that the required IRR for $\mathcal{G}$ should correspond to the $k_z=0$ plane of the 3D Brillouin zone (BZ). Similarly, for a MRG describing a 1D system along z, the IRR for $\mathcal{G}$ should correspond to the $k_x=k_y=0$ path of the BZ.

There is another technical issue arising in practical calculations. Usually, the coordinate system for the standard setting of a magnetic space group, as in well-known references, is different from the $\mathcal{G}$ constructed here. The two generally differ by a proper rotation and a shift of origin. Thus, in order to use the documented IRRs for magnetic space groups, we need to align the two coordinate systems.

Let $\mathsf{L}=(\boldsymbol{a},\boldsymbol{b},\boldsymbol{c})$ be lattice vectors for the $\mathcal{G}$ constructed from $\mathcal{S}$ and $\mathsf{L}'=(\boldsymbol{a}',\boldsymbol{b}',\boldsymbol{c}')$ be lattice vectors in the standard setting for this space group. The two sets of lattice vectors differ by a linear transformation Q:

$$\mathsf{L}=\mathsf{L}'Q,\tag{6}$$

where Q is a 3×3 matrix and $\det Q=1$ and is determined by $Q=\mathsf{L}\mathsf{L}'^{-1}$.

Besides the rotation, the two coordinate systems may have a shift in origin. Consider a general point labeled by coordinate $\boldsymbol{x}$ in the L system. Its coordinate in L' is given by

$$\boldsymbol{x}'=Q\boldsymbol{x}+\boldsymbol{\ell},\tag{7}$$

where $\boldsymbol{\ell}$ is the shift of origin between the two coordinate system. This shift enters into the expression of general space group symmetry operation. Considering the expression of any space group symmetry operation, we should have

$$\{R'|\boldsymbol{\tau}'\}=\{QRQ^{-1}|Q\boldsymbol{\tau}-QRQ^{-1}\boldsymbol{\ell}+\boldsymbol{\ell}\}.\tag{8}$$

In our current case, we already know the lattice vectors L and L' and the expressions $\{R_i|\boldsymbol{\tau}_i\}$ and $\{R_i'|\boldsymbol{\tau}_i'\}$ (i labels the symmetry generators). The target is to solve out $\boldsymbol{\ell}$. This is done by using the following algorithm.

We write down the following set of equations obtained from (8):

$$\boldsymbol{\tau}_i'=Q\boldsymbol{\tau}_i-QR_iQ^{-1}\boldsymbol{\ell}+\boldsymbol{\ell}\pmod 1,\tag{9}$$

where the lattice periodicity allows the two sides differing by a lattice period. Note that this set of equations is not conventional linear congruence equations, since $\boldsymbol{\tau}_i'$, $\boldsymbol{\tau}_i$, and $\boldsymbol{\ell}$ can be fractional numbers. We can multiply Eq. (9) by integer N to turn them into linear congruence equations

$$N\boldsymbol{\tau}_i'=Q(N\boldsymbol{\tau}_i)-QR_iQ^{-1}(N\boldsymbol{\ell})+(N\boldsymbol{\ell})\pmod N,\tag{10}$$

where N is the least common multiple of the denominators of $\boldsymbol{\tau}_i'$, $\boldsymbol{\tau}_i$, and $\boldsymbol{\ell}$. Here, although we do not yet know the denominator of $\boldsymbol{\ell}$, in space groups, it will not be a large integer. In fact, from our calculation, the maximum N is just 12. Therefore, in practice, one may just try to increasingly select a N, solve $\boldsymbol{\ell}$ from (10) by using the Chinese remainder theorem [53], and check whether such a solution is valid.

The whole process for obtaining the IRRs of a subperiodic group $\mathcal{S}$ is schematically illustrated in Fig. 1.

TABLE II. Emergent particles in MRGs. The format of this table is similar to Table I.

Notation	Abbr.	d_m	d	Ld	I	II	III	IV
MRGs w/o spin								
Weyl point	WP	0	2	(1)	√	√	√	√
Triple point	TP	0	3	(1)	√	√	√	√
Dirac point	DP	0	4	(1)	√	√	√	√
MRGs w/ spin								
Weyl point	WP	0	2	(1)	√	√	√	√
Triple point	TP	0	3	(1)	√	√	√	√
Dirac point	DP	0	4	(1)	√	√	√	√

III. CLASSIFICATION OF EMERGENT PARTICLES

After deriving the IRRs of a given MLG or MRG, we can use them to identity possible band degeneracies and the associated emergent particles. The remaining steps are exactly the same as our previous works in Refs. [33,34] on the classification for magnetic space groups.

For emergent particles around a degeneracy point $\boldsymbol{k}$ in BZ, we construct the $k \cdot p$ effective models constrained by symmetry conditions:

$$H(\boldsymbol{k}) = \begin{cases} D(S)H(R^{-1}\boldsymbol{k})D^{-1}(S), & \text{if } S = \{R|\boldsymbol{\tau}\}, \\ D(S)H^*(-R^{-1}\boldsymbol{k})D^{-1}(S), & \text{if } S = \{R|\boldsymbol{\tau}\}\mathcal{T}, \end{cases} \tag{11}$$

where the rotation part of S will run through all symmetry generators in the magnetic little cogroup at $\boldsymbol{k}$, D is its representation corresponding to the band degeneracy, and $\mathcal{T}$ is the time reversal operation. We have developed a general algorithm to construct such effective models and implemented it in the MagneticKP package, as introduced in Ref. [54].

The main results from our classification are summarized in Table I (for MLGs) and Table II (for MRGs). In the first column, we list the kinds of emergent particles that are protected by MLGs or MRGs. In Refs. [25,33,34], we showed that there are 27 kinds of emergent particles protected by magnetic space groups in 3D. Here, for MLGs and MRGs, due to the reduced symmetry, we find that the variety of particles is also much reduced. In MLGs, there are six kinds of particles, corresponding to (linear) Weyl point, quadratic Weyl point, cubic Weyl point, Dirac point, Weyl line, and Dirac line. In the naming, we use Weyl and Dirac to indicate the number of degeneracy to be 2 and 4, respectively, consistent with the convention in Refs. [25,33,34]. For MRGs, there are only three kinds of emergent particles, which correspond to Weyl point, triple point, and Dirac point. Some basic characters of these band degeneracies, such as the dimension, the degree of degeneracy, and the leading order band splitting, are also listed in Tables I and II.

The remaining columns of Tables I and II show the possible appearance of a kind of emergent particle in the four types of MLGs or MRGs.

The type-II MLGs and MRGs describe the nonmagnetic 2D and 1D crystals, which cover most existing materials. Taking them as examples, we list the candidate type-II MLGs and MRGs that host each kind of emergent particle in Table III (for MLGs) and IV (for MRGs).

In the Supplemental Material [49], we present the following detailed information. For each kind of emergent particle, we list all MLGs or MRGs that can host it. For each MLG or MRG, we list the band degeneracies it can have, their locations in BZ, the symmetry generators, their representations, and the effective models. The format of such a dictionary follows the convention set in Ref. [34].

We have a few remarks before proceeding. First, the well-known double degeneracy for all points in BZ due to the space-time inversion symmetry $\mathcal{PT}$ for spinful systems is not counted in our classification. Second, most degeneracies occur on high-symmetry points or high-symmetry paths of BZ. However, there are three mechanisms that can protect Weyl point or Weyl lines at generic points of BZ. (i) Spinless MLGs with $\mathcal{PT}$ symmetry can protect Weyl points at generic k points. (ii) Spinless or spinful MLGs with $C_{2z}\mathcal{T}$ symmetry can protect Weyl points at generic k points. (iii) MLGs with a horizontal mirror plane can protect Weyl lines passing through generic k points. For these cases, one needs to carefully scan the BZ when looking for band degeneracies.

TABLE III. List of type-II MLGs that host each kind of emergent particle.

Name	Layer groups
W/o spin	
LWP	8–10,14–48,53–64,66–73,75–80
QWP	49–80
DP	29,33,40,43–45,63
WL	5,7,9,12,15–17,20–21,24–25,27–48,51–52,54,56,58 60–64,74–75,78–80
WLs	7,21,25,32,34,39,42,44,46,52,54,56,58,60,62–64
W/ spin	
LWP	1,3,5,8–13,19–26,31–34,36,49–50,53–60,65,67–70 73,76–77
CWP	65,67–70,73,76–77
DP	7,15–17,21,25,28–30,32–34,38–39,41–43,45–46,48,52 54,56,58,60,62,64
WL	4–5,9,12,17,20–21,24–25,27–36,54,56,58,60,74,78–79
WLs	74,78,79
DL	40,43,44,45,63
DLs	44,63

TABLE IV. List of type-II MRGs that host each kind of emergent particle.

Name	Rod groups
W/o spin	
WP	5,7–9,11–26,28–44,46–58,60–75
TP	27–29,34–41,45,49–52,59–61,68–75
DP	36,40,50,52,60,61,68–70,72–75
W/ spin	
WP	1,3–5,8–10,13,14,18,19,23–26,30–33,42–44,46–50,53–59 62–67,71,72
TP	49,50,59,71,72
DP	7,12,16,17,21,22,28,29,34–36,38–41,45,50–52,60,61 68–70,72–75

IV. DISCUSSION AND CONCLUSION

It is worth mentioning that the spinful quadratic Weyl point, which was found not existing in type-II MLGs, can exist in type-I and type-III MLGs, as shown in Table I. For example, consider the type-III MLG $p\bar{6}'$ (no. 74.3.494). The corepresentation matrices for two symmetry generators C_{3z} and $\sigma_h\mathcal{T}$ in the basis of $\Gamma_4\Gamma_5$ degeneracy are

$$D(C_{3z}) = e^{i\pi\sigma_3/3}, \quad D(\sigma_h\mathcal{T}) = \sigma_1, \tag{12}$$

where σ_i's are the Pauli matrices. Then the effective model for states around the $\Gamma_4\Gamma_5$ degeneracy is

$$H(\boldsymbol{k}) = c_1\left(k_x^2 + k_y^2\right) + [(c_2k_-^2 + c_3k_+^2)\sigma_+ + \text{H.c.}], \tag{13}$$

where the momentum and the energy are measured from the degeneracy point and the c_i's are real-valued parameters. This model confirms that the degeneracy point is a quadratic Weyl point in a spinful system. Furthermore, for MLG $p\bar{6}'$, this quadratic Weyl point can be the only Fermi point of a band structure. To show this, we construct a tight-binding model on a hexagonal lattice as shown in Figs. 2(a) and 2(b). Here, each active site (marked by red color) has two s-like orbitals $\{|s\uparrow\rangle, |s\downarrow\rangle\}$. The gray colored sites are added to enforce the proper MLG, but they do not contain active orbitals. We construct the following model that satisfies the $p\bar{6}'$ symmetry [55]:

$$H(\boldsymbol{k}) = \varepsilon + \begin{pmatrix} \boldsymbol{\alpha}_1\cdot(t_1\boldsymbol{A} + t_2\boldsymbol{B}) & \boldsymbol{\alpha}_2\cdot t_3\boldsymbol{A} \\ \dagger & \boldsymbol{\alpha}_1\cdot(t_1\boldsymbol{A} - t_2\boldsymbol{B}) \end{pmatrix}, \tag{14}$$

where the bold symbols are vectors, $\boldsymbol{\alpha}_1 = (1,1,1)$, $\boldsymbol{\alpha}_2 = (e^{-\frac{i\pi}{6}}, -e^{\frac{i\pi}{6}}, i)$, $\boldsymbol{A} = [\cos k_a, \cos k_b, \cos(k_a + k_b)]$, $\boldsymbol{B} = [\sin k_a, \sin k_b, \sin(k_a + k_b)]$, k_a and k_b are wave vector components along the two reciprocal lattice vectors, and $\varepsilon, t_1, t_2, t_3$ are real parameters. The resulting band structure in Figs. 2(b) and 2(c) demonstrates our claim. Interestingly, when one adds an extra horizontal mirror σ_h to the system, the type-III MLG $p\bar{6}'$ is turned into the type-II MLG $p\bar{6}1'$. The Weyl point at Γ will no longer be an isolated nodal point, but sit on the intersection of three nodal loops, as illustrated in Fig. 2(d).

We find that the cubic Weyl point can exist in spinful type-II MLGs, consistent with the prediction in Ref. [56]. In addition, our result shows that it also exists in spinful type-I MLGs, but not in type-III and type-IV MLGs. This can be understood from the following analysis. A cubic Weyl point necessarily requires one of these six symmetry groups generated by $\{C_3, \mathcal{T}\}$, $\{C_6, \mathcal{T}\}$, $\{C_6, C_{21}\}$, $\{C_6, C_{21}, \mathcal{T}\}$, $\{C_6, \sigma_d\}$, and $\{C_6, \sigma_d, \mathcal{T}\}$, respectively, where C_{21} and σ_d are rotation and mirror perpendicular to the C_6 axis. It turns out that the index 2 subgroup of above six magnetic point groups cannot be a type-III magnetic point group, indicating that the type-III MLGs cannot host a cubic point. Moreover, if a type-IV MLG can host the cubic point, the combination of a half lattice translation and $\mathcal{T}$ must be compatible with the C_3 symmetry. However, the relation $C_3\{\mathcal{T}|\frac{1}{2}0\}C_3^{-1} = \{\mathcal{T}|0\frac{1}{2}\}$ (or $C_3\{\mathcal{T}|\frac{1}{2}\frac{1}{2}\}C_3^{-1} = \{\mathcal{T}|\frac{1}{2}0\}$) will give rise to an invalid symmetry element $\{E|\frac{1}{2}\frac{1}{2}\}$ (or $\{E|0\frac{1}{2}\}$). Therefore, cubic Weyl points also cannot exist in type-IV MLGs.

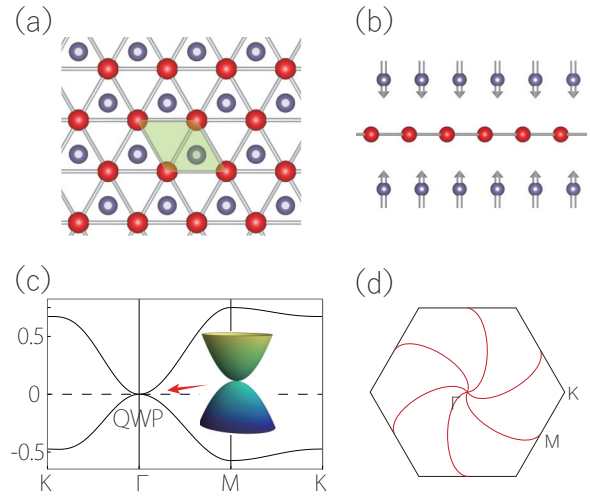

FIG. 2. (a) Top view and (b) side view of our constructed QWP lattice model. The green shaded region indicates the unit cell. The active orbitals are at the red colored sites. The gray colored sites with local magnetic moments are added to enforce the proper MLG symmetry. (c) Band structure of the model (14). In the calculation, we take $\varepsilon = 0.06$, $t_1 = -0.02$, $t_2 = 0.2$, and $t_3 = -0.3$. Inset shows the dispersion around the QWP. (d) After adding a horizontal mirror to the model, the MLG changes to the type-II MLG $p\bar{6}1'$. Then there appears three WLs as indicated by the red lines.

Although the number of kinds of emergent particles in MRGs is less than that in MLGs, we find that the triple points can exist in MRGs but not in MLGs. Triple points have been extensively studied in 3D systems. In magnetic space groups, they may appear as essential degeneracies at high-symmetry points. However, this is possible only in cubic system, and we find that such triple points cannot be maintained when restricting to 2D or 1D subperiodic systems. Another possibility to form a triple point is by crossing a doubly degenerate band with a nondegenerate band, corresponding to a direct sum of a 1D corepresentation and a 2D corepresentation on a high symmetry line or plane. In MLGs, this has to be on a high-symmetry path of 2D BZ. The little cogroup $\mathcal{L}$ on this path should be one from C_1, C_2, C_s, and C_{2v}. By using the property of characters

$$\sum_i \chi_i^2(e) = |\mathcal{L}|, \tag{15}$$

where e is the identity element and the sum is over all IRRs. One finds that, for the four little cogroups, the dimensions of IRRs are either all 1 or all 2. Therefore, it is impossible to generate a triple point. When taking antiunitary operations into account, one can show that the dimensions of corepresentations are either unchanged or multiplied by 2. Thus MLGs cannot host triple points but can host Dirac points and Dirac lines. By contrast, MRGs can have other rotational symmetries (such as C_3, C_4, C_6) in addition to C_2 along its periodic direction. Therefore, these additional symmetries can enable triple points in MRGs.

It must be noted that MRGs are defined as subperiodic groups of magnetic space groups. They only contain symmetries that are inherited from 3D crystals. However, for 1D or quasi-1D crystals, they may have symmetries that do not exist for 3D crystals. For example, one can easily picture a 1D crystal with C_5 symmetry or even C_∞ symmetry. The groups that capture all these possibilities are known as the line groups [57,58]. Our study here can be extended to line groups in the near future.

In conclusion, we systematically classify the emergent particles in 528 MLGs and 394 MRGs. In the process, we develop a general approach to derive all IRRs of a subperiodic group by constructing a corresponding superperiodic group and by properly restricting the IRRs of the superperiodic group. This approach is applied to obtain all IRRs of MLGs and MRGs. Using these IRRs, we established an encyclopedia of emergent particles in MLGs and MRGs. It can serve as a valuable reference for the search of novel emergent particles in lower dimensional materials. It can also be used to facilitate the design of artificial crystals to study the fascinating properties of emergent particles.

ACKNOWLEDGMENTS

The authors thank D. L. Deng for helpful discussions. We acknowledge support from the NSF of China (Grant No. 12234003), the National Key R&D Program of China (Grant No. 2020YFA0308800), the NSF of China (Grants No. 12004028, No. 12004035, No. 12274028, No. 52161135108, and No. 12061131002), and the Singapore MOE AcRF Tier 2 (Grant No. MOE-T2EP50220-0011). W.W. is supported by the Guangdong Basic and Applied Basic Research Foundation (Grant No. 2022A1515110094) and the Special Funding in the Project of Qilu Young Scholar Program of Shandong University.

[1] C.-K. Chiu, J. C. Y. Teo, A. P. Schnyder, and S. Ryu, Rev. Mod. Phys. **88**, 035005 (2016).
[2] A. A. Burkov, Nat. Mater. **15**, 1145 (2016).
[3] N. P. Armitage, E. J. Mele, and A. Vishwanath, Rev. Mod. Phys. **90**, 015001 (2018).
[4] X. Wan, A. M. Turner, A. Vishwanath, and S. Y. Savrasov, Phys. Rev. B **83**, 205101 (2011).
[5] S. M. Young, S. Zaheer, J. C. Y. Teo, C. L. Kane, E. J. Mele, and A. M. Rappe, Phys. Rev. Lett. **108**, 140405 (2012).
[6] Z. Wang, Y. Sun, X.-Q. Chen, C. Franchini, G. Xu, H. Weng, X. Dai, and Z. Fang, Phys. Rev. B **85**, 195320 (2012).
[7] L. Lu, J. D. Joannopoulos, and M. Soljačić, Nat. Photon. **8**, 821 (2014).
[8] Z. Yang, F. Gao, X. Shi, X. Lin, Z. Gao, Y. Chong, and B. Zhang, Phys. Rev. Lett. **114**, 114301 (2015).
[9] T. Ozawa, H. M. Price, A. Amo, N. Goldman, M. Hafezi, L. Lu, M. C. Rechtsman, D. Schuster, J. Simon, O. Zilberberg, and I. Carusotto, Rev. Mod. Phys. **91**, 015006 (2019).
[10] J. Ningyuan, C. Owens, A. Sommer, D. Schuster, and J. Simon, Phys. Rev. X **5**, 021031 (2015).
[11] S. Imhof, C. Berger, F. Bayer, J. Brehm, L. W. Molenkamp, T. Kiessling, F. Schindler, C. H. Lee, M. Greiter, T. Neupert, and R. Thomale, Nat. Phys. **14**, 925 (2018).
[12] R. Yu, Y. X. Zhao, and A. P. Schnyder, Natl. Sci. Rev. **7**, 1288 (2020).
[13] S. D. Huber, Nat. Phys. **12**, 621 (2016).
[14] G. Ma, M. Xiao, and C. T. Chan, Nat. Rev. Phys. **1**, 281 (2019).
[15] S. A. Yang, H. Pan, and F. Zhang, Phys. Rev. Lett. **113**, 046401 (2014).
[16] H. Weng, Y. Liang, Q. Xu, R. Yu, Z. Fang, X. Dai, and Y. Kawazoe, Phys. Rev. B **92**, 045108 (2015).
[17] K. Mullen, B. Uchoa, and D. T. Glatzhofer, Phys. Rev. Lett. **115**, 026403 (2015).
[18] Y. Chen, Y. Xie, S. A. Yang, H. Pan, F. Zhang, M. L. Cohen, and S. Zhang, Nano Lett. **15**, 6974 (2015).
[19] C. Zhong, Y. Chen, Y. Xie, S. A. Yang, M. L. Cohen, and S. B. Zhang, Nanoscale **8**, 7232 (2016).
[20] Q.-F. Liang, J. Zhou, R. Yu, Z. Wang, and H. Weng, Phys. Rev. B **93**, 085427 (2016).
[21] W. Wu, Y. Liu, S. Li, C. Zhong, Z.-M. Yu, X.-L. Sheng, Y. X. Zhao, and S. A. Yang, Phys. Rev. B **97**, 115125 (2018).
[22] J. L. Mañes, Phys. Rev. B **85**, 155118 (2012).
[23] Z. Zhu, G. W. Winkler, Q. S. Wu, J. Li, and A. A. Soluyanov, Phys. Rev. X **6**, 031003 (2016).
[24] B. Bradlyn, J. Cano, Z. Wang, M. G. Vergniory, C. Felser, R. J. Cava, and B. A. Bernevig, Science **353**, aaf5037 (2016).
[25] Z.-M. Yu, Z. Zhang, G.-B. Liu, W. Wu, X.-P. Li, R.-W. Zhang, S. A. Yang, and Y. Yao, Sci. Bull. **67**, 375 (2022).
[26] C. Fang, M. J. Gilbert, X. Dai, and B. A. Bernevig, Phys. Rev. Lett. **108**, 266802 (2012).
[27] G. Xu, H. Weng, Z. Wang, X. Dai, and Z. Fang, Phys. Rev. Lett. **107**, 186806 (2011).
[28] Z.-M. Yu, W. Wu, X.-L. Sheng, Y. X. Zhao, and S. A. Yang, Phys. Rev. B **99**, 121106(R) (2019).
[29] Z. Zhang, Z.-M. Yu, and S. A. Yang, Phys. Rev. B **103**, 115112 (2021).
[30] C. Cui, X.-P. Li, D.-S. Ma, Z.-M. Yu, and Y. Yao, Phys. Rev. B **104**, 075115 (2021).
[31] C. Bradley and A. Cracknell, *Mathematical Theory of Symmetry in Solids: Representation Theory for Point Groups and Space Groups*, Oxford Classic Texts in the Physical Sciences (Oxford University Press, Oxford, 2009).
[32] F. Tang and X. Wan, Phys. Rev. B **104**, 085137 (2021).

[33] G.-B. Liu, Z. Zhang, Z.-M. Yu, S. A. Yang, and Y. Yao, Phys. Rev. B **105**, 085117 (2022).
[34] Z. Zhang, G.-B. Liu, Z.-M. Yu, S. A. Yang, and Y. Yao, Phys. Rev. B **105**, 104426 (2022).
[35] F. Tang and X. Wan, Phys. Rev. B **105**, 155156 (2022).
[36] Y. Xia, P. Yang, Y. Sun, Y. Wu, B. Mayers, B. Gates, Y. Yin, F. Kim, and H. Yan, Adv. Mater. **15**, 353 (2003).
[37] P. Miró, M. Audiffred, and T. Heine, Chem. Soc. Rev. **43**, 6537 (2014).
[38] C. Tan, X. Cao, X.-J. Wu, Q. He, J. Yang, X. Zhang, J. Chen, W. Zhao, S. Han, G.-H. Nam, M. Sindoro, and H. Zhang, Chem. Rev. **117**, 6225 (2017).
[39] A. H. Castro Neto, F. Guinea, N. M. R. Peres, K. S. Novoselov, and A. K. Geim, Rev. Mod. Phys. **81**, 109 (2009).
[40] X. Feng, J. Zhu, W. Wu, and S. A. Yang, Chin. Phys. B **30**, 107304 (2021).
[41] S. Park and B.-J. Yang, Phys. Rev. B **96**, 125127 (2017).
[42] N. Lazić, V. Damljanović, and M. Damnjanović, J. Phys. A: Math. Theor. **55**, 325202 (2022).
[43] M. Damnjanović, I. Milošević, and M. Vujičić, Phys. Rev. B **39**, 4610 (1989).
[44] M. Damnjanović and I. Milosević, Phys. Rev. B **43**, 13482 (1991).
[45] D. B. Litvin and T. R. Wike, *Character Tables and Compatibility Relations of The Eighty Layer Groups and Seventeen Plane Groups* (Springer US, Boston, MA, 1991).
[46] B. Nikolić, I. Milošević, T. Vuković, N. Lazić, S. Dmitrović, Z. Popović, and M. Damnjanović, Acta Crystallogr., A: Found. Adv. **78**, 107 (2022).
[47] J. Laurens and M. Boon, *Theory of Finite Groups: Applications in Physics* (North-Holland, Amsterdam, 1967).
[48] D. B. Litvin, *Magnetic Subperiodic Groups and Magnetic Space Groups* (Wiley Online Library, 2016).
[49] See Supplemental Material at http://link.aps.org/supplemental/10.1103/PhysRevB.107.075405 for correspondence between magnetic subperiodic groups and magnetic space groups, quantitative mapping of magnetic subperiodic groups and emergent particles, and detailed tables of the emergent particles for each magnetic subperiodic group.
[50] G.-B. Liu, M. Chu, Z. Zhang, Z.-M. Yu, and Y. Yao, Comput. Phys. Commun. **265**, 107993 (2021).
[51] G.-B. Liu, Z. Zhang, Z.-M. Yu, and Y. Yao, arXiv:2211.10740.
[52] G. D. James and M. W. Liebeck, *Chapter17, Theorem 17.3, Representations and Characters of Groups*, 2nd ed. (Cambridge University Press, Cambridge, UK, 2001).
[53] M. Artin, *Algebra* (Pearson Education, London, 2011).
[54] Z. Zhang, Z.-M. Yu, G.-B. Liu, Z. Li, S. A. Yang, and Y. Yao, arXiv:2205.05830.
[55] Z. Zhang, Z.-M. Yu, G.-B. Liu, and Y. Yao, Comput. Phys. Commun. **270**, 108153 (2022).
[56] W. Wu, Y. Liu, Z.-M. Yu, Y. X. Zhao, W. Gao, and S. A. Yang, arXiv:2105.08424.
[57] M. Damnjanović and M. Vujičić, Phys. Rev. B **25**, 6987 (1982).
[58] M. Damnjanović, I. Milosevic, and I. Milošević, *Line Groups in Physics: Theory and Applications to Nanotubes and Polymers*, Lecture Notes in Physics (Springer, Berlin, 2010).